Plasmon excitations in a two-dimensional electron gas with spin-orbit interactions: Zero magnetic field

M. S. Kushwaha[1] and S. E. Ulloa[2]
[1]*Institute of Physics, University of Puebla, P.O. Box J-45, Puebla 72570, Mexico*
[2]*Department of Physics and Astronomy, and Nanoscale and Quantum Phenomena Institute, Ohio University, Athens, Ohio 45701-2979, USA*

(Received 13 September 2005; revised manuscript received 22 December 2005; published 3 May 2006)

We report on a theoretical investigation of plasmon excitations in a quasi-two-dimensional electron gas in the presence of a spin-orbit (SO) interaction induced by the Rashba effect. We derive and discuss the dispersion relations for both intra-SO and inter-SO charge-density excitations within the framework of the Bohm-Pines random-phase approximation. The zero-field (or Rashba) spin splitting gives rise to *three* branches of plasmon excitations, even when only the lowest electric subband is occupied. However, not all three plasmon branches survive the Landau damping as is discussed in detail. It is found that, in the long-wavelength limit, the two branches of inter-SO plasmons are optic-like, propagate with negative group velocity, and remain stronger functions of the Rashba parameter than their intra-SO counterpart. We discuss the dependence of the plasmon energy on the propagation vector, the two-dimensional charge density, and the effective Rashba wave vector.

DOI: 10.1103/PhysRevB.73.205306 PACS number(s): 73.20.Mf, 72.25.Dc, 71.70.Ej, 75.25.+z

I. INTRODUCTION

The continued tremendous amount of research interest focused on miniaturization (of size and dimensions), leading to such manmade systems as quantum wells, wires, and dots,[1] has in recent years evolved into the study of narrow-gap semiconductors, most notably InAs, and the important role they play in the rapidly evolving field of *spintronics*.[2] Spintronics is based on the concept of exploiting the spin degree of freedom of the carriers to develop novel features and functionalities for solid-state devices. As a nonmagnetic element in hybrid devices, these semiconductor materials are expected to help control the electron spin states just as the electron charge is controlled in conventional electronic devices. One key idea of such devices is that the spin-orbit interaction (SOI) in narrow-gap semiconductors causes the spins of the carriers to precess. This was conceived by Datta and Das in a seminal paper,[3] which describes how the external gate electrode can be used to manipulate the SOI provided that the latter is dependent on the interface electric field, the so-called Rashba effect.[4]

In the present paper, we investigate the electron spin dynamics in $In_{1-x}Ga_xAs/In_{1-x}Al_xAs$ quantum wells within the lowest occupied (electric) subband in the framework of the Bohm-Pines random-phase approximation (RPA). It is now well known, both theoretically[5] and experimentally,[6] that in such narrow-gap semiconductors there is energy splitting between spin-up and spin-down electrons even when there is *no* magnetic field (while preserving the Kramers degeneracy). Also, it is now generally accepted that the SOI in this "zero-field spin splitting" is governed by the Rashba Hamiltonian, which increases linearly with the electron wave vector.[2] One of the motivations behind this work is that the Rashba Hamiltonian turns out to yield, via intra-SO and inter-SO transistions, plasmon frequencies in the terahertz regime in which many promising new devices, such as modulators,[7] detectors,[8] and quantum lasers,[9] operate. As such, it seems worthwhile to explore the electron spin dynamics as a possible route towards novel applications in the terahertz regime.[10–12]

Quite recently there have been reported a few works that deal with the Rashba effect on the intrasubband plasmon dispersion in the two-dimensional electron gas (2DEG).[13–15] Reference 13 reported approximate (in the long-wavelength limit) plasmon dispersion using the Green-function method, with no physical explanation whether or not the three plasmon branches survive the Landau damping. Reference 14 reports a single plasmon branch and intra-SO and inter-SO single-particle regions using (admittedly) a different dielectric function. Reference 14 emphasizes that the only plasmon branch reported there suffers from Landau damping inside the upper (inter-SO) single-particle region. This is a misconception and misinterpretation of well-known aspects related with the Landau damping of a certain plasmon mode. This is because the existence of this upper single-particle region is *equivalent* to the intersubband single-particle excitation (SPE) region in a, say, two-subband model (in the absence of any SOI), and it is well known that in that case the *intrasubband* plasmon only suffers from the Landau damping as and when it merges with the respective SPE region; it does not suffer from the Landau damping whether or not it crosses the *intersubband* SPE region, more so because the intrasubband and intersubband plasmons (and their respective SPE regions) are, by definition, two different modes of excitation bearing different mechanisms, particularly when the confining potential is symmetric and hence there is *no* coupling between the two, just as is the case studied in Ref. 14. To be more explicit, one can notice that the only (intra-SO) plasmon branch shown in Ref. 14 goes through the upper (inter-SO) SPE region quite unperturbed. Reference 15 is, to our knowledge, the latest effort dedicated to study the plasmon dispersion in a 2DEG with SOI in the linear response formalism. It is interesting to note that all these three works[13–15] remain somewhat inconsistent (with each other) with respect

to the number and propagation characteristics of the plasmon branches existing in a 2DEG with a spin-orbit interaction. This work, where we present the full RPA formalism as well as a detailed numerical analysis of the plasmon dispersion in a 2DEG with Rashba SOI, will clarify issues relevant to the collective excitations, single-particle excitations, and the Landau damping.

The rest of the paper is organized as follows. In Sec. II we present our mathematical formalism for the two-dimensional electron gas in the presence of the SOI and derive briefly the required nonlocal, dynamic dielectric function within the RPA. Section III is devoted to discuss our numerical results for the plasmon excitations for the several case studies. We conclude our finding with a discussion in Sec. IV.

II. MATHEMATICAL FORMALISM

For a typical two-dimensional electron gas in the x-y plane in narrow-gap semiconductors, such as $In_{1-x}Ga_xAs/In_{1-x}Al_xAs$ quantum wells, the single-electron Hamiltonian including the lowest-order of the spin-orbit interaction can be expressed as

$$H = \frac{\hat{\mathbf{p}}^2}{2m^*} + \frac{\alpha}{\hbar}(\hat{\boldsymbol{\sigma}} \times \hat{\mathbf{p}})_z + V_c(z), \tag{1}$$

where α is the Rashba parameter, which describes the strength of the SOI, $\hat{\sigma} \equiv (\sigma_x, \sigma_y, \sigma_z)$ stands for the Pauli spin matrices, $\hat{\mathbf{p}}$ is the momentum operator, and the rest of the symbols have their usual meanings. We assume the electrons to be confined in a zero-thickness x-y plane due to a relatively stronger confinement potential $V_c(z)$. This is expected to be a reasonably good approximation for low electron densities (at low temperatures) when only the lowest 2D subband in a quantum well is occupied by electrons. Such a system is characterized by the eigenfunctions

$$\psi_\zeta(\mathbf{x}) = \frac{1}{\sqrt{2}} e^{i\mathbf{k}\cdot\mathbf{r}} \phi_n(z) \begin{pmatrix} 1 \\ \sigma\beta \end{pmatrix}, \tag{2}$$

where $\mathbf{r}$ ($\mathbf{k}$) is a 2D vector in the direct (reciprocal) space, $\sigma = \pm 1$ refers to the spin-up and spin-down states, and $\beta = (k_y - ik_x)/k$, and the eigenenergies are

$$E_k^\sigma = \frac{\hbar^2}{2m^*}[k^2 + 2\sigma k_\alpha k] + \epsilon_n, \tag{3}$$

where $k_\alpha = \alpha m^*/\hbar^2$ is the effective Rashba wave vector. Note that the normalization factor in Eq. (2) is such that the area of the 2DEG $S=1$. In Eq. (3), ϵ_n is the energy of the nth subband. The important characteristic of this dispersion relation is that the spins are degenerate at $k=0$ and the spin splitting increases linearly with k. This is clearly demonstrated in Fig. 1 which shows the plot of Eq. (3), with $\epsilon_n = 0$.

We start with a general expression for the single-particle density-density response function $\chi^0(\cdots)$ (Ref. 1):

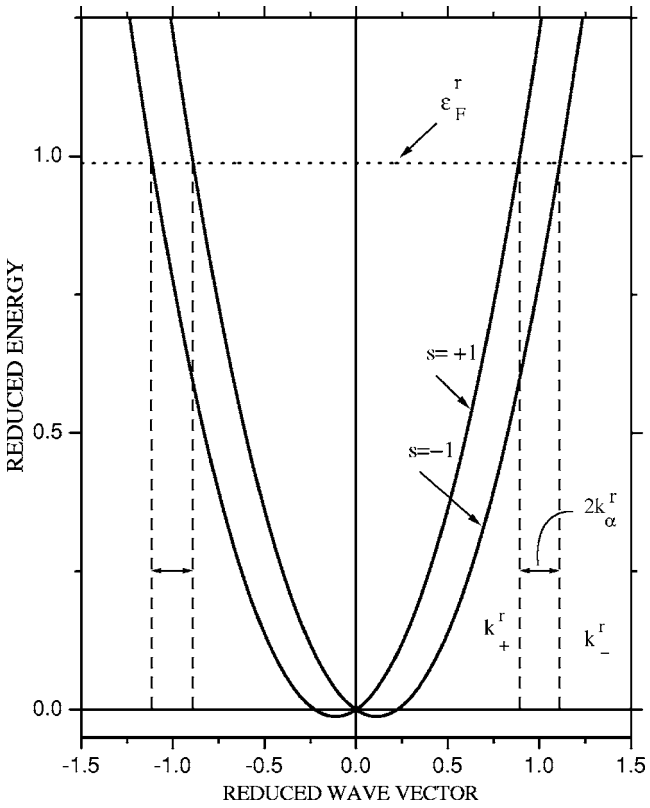

FIG. 1. Spin-orbit induced subbands of an isotropic 2DEG [Eq. (3)]. ϵ_F^r is the reduced Fermi energy, and k_+^r and k_-^r are the reduced wave vectors for the upper ($s=+1$) and lower ($s=-1$) branches, respectively. $k_+^r - k_-^r = 2k_\alpha^r$; $T=0$ K. The value of $E^\pm(k)$ reaches a minimum on a circle, which is a loop of extrema. The radius of this circle is k_α, and we have $E^{\mp} = \Delta = \pm \alpha k_\alpha/2$.

$$\chi^0(\mathbf{x}, \mathbf{x}'; \omega) = \sum_{ij} \frac{f(\epsilon_i) - f(\epsilon_j)}{\epsilon_i - \epsilon_j + \hbar\omega^*} \psi_i^*(\mathbf{x}') \psi_j(\mathbf{x}') \psi_j^*(\mathbf{x}) \psi_i(\mathbf{x}). \tag{4}$$

For all practical purposes, this equation takes the following form ($\mathbf{x} \equiv \{\mathbf{r}, z\}, \xi$):

$$\chi^0(\mathbf{x}, \mathbf{x}'; \omega) = \sum_{\zeta\zeta'} \Lambda_{\zeta\zeta'} \psi_\zeta^*(\mathbf{x}') \psi_{\zeta'}(\mathbf{x}') \psi_{\zeta'}^*(\mathbf{x}) \psi_\zeta(\mathbf{x}), \tag{5}$$

where $\zeta \equiv \{\{\mathbf{k}, n\}, \sigma\}$ is a composite index and $\Lambda_{\zeta\zeta'}$ is defined as

$$\Lambda_{\zeta,\zeta'} \equiv \Lambda_{nn'}^{\sigma\sigma'} = \frac{f(\epsilon_{n\mathbf{k}}^\sigma) - f(\epsilon_{n'\mathbf{k}'}^{\sigma'})}{\epsilon_{n\mathbf{k}}^\sigma - \epsilon_{n'\mathbf{k}'}^{\sigma'} + \hbar\omega^*}, \tag{6}$$

where $\omega^* = \omega + i\gamma$ and small but nonzero γ represents the adiabatic switching of the Coulomb interactions in the remote past. Next, we write Eqs. (2) symbolically as follows:

$$\psi_\zeta(\mathbf{x}) = \psi_{\mathbf{k}}(\mathbf{r}) \phi_n(z) \chi_\sigma(\xi), \tag{7}$$

where

$$\phi_{\mathbf{k}}(\mathbf{r}) = \frac{1}{\sqrt{2}} e^{i\mathbf{k}\cdot\mathbf{r}} \text{ and } \chi_\sigma(\xi) = \begin{pmatrix} 1 \\ \sigma\beta \end{pmatrix}. \tag{8}$$

As such, we cast Eq. (5) in the following convenient form:

$$\chi^0(\mathbf{x},\mathbf{x}';\omega) = \sum_{\sigma\sigma'} \sum_{nn'} \sum_{\mathbf{k}k'} \Lambda_{nn'}^{\sigma\sigma'}(\mathbf{k},\mathbf{k}') e^{i\mathbf{q}\cdot(\mathbf{r}'-\mathbf{r})} \times \phi_n^*(z')\phi_{n'}(z')\phi_{n'}^*(z)\phi_n(z)\chi_\sigma^*\chi_{\sigma'}\chi_{\sigma'}^*\chi_\sigma. \tag{9}$$

Here $\mathbf{q}=\mathbf{k}'-\mathbf{k}$ is the 2D momentum transfer in the x-y plane. Since the translational invariance does persist in the 2D plane, we can Fourier-transform this equation with respect to $\mathbf{r}$. For this purpose, we multiply both sides of this equation by $e^{-i\mathbf{q}'\cdot(\mathbf{r}'-\mathbf{r})}$ and integrate over r', resulting in

$$\chi^0(\mathbf{q},\omega;z,z') = \sum_{\sigma\sigma'} \sum_{nn'} \sum_{\mathbf{k}} \Lambda_{nn'}^{\sigma\sigma'}(\mathbf{k},\mathbf{k}'=\mathbf{k}+\mathbf{q}) \times \phi_n^*(z')\phi_{n'}(z')\phi_{n'}^*(z)\phi_n(z)\chi_\sigma^*\chi_{\sigma'}\chi_{\sigma'}^*\chi_\sigma. \tag{10}$$

The induced particle density is defined in terms of Kubo's correlation function by

$$n_{in}(\mathbf{q},\omega;z) = \int dz' \chi^0(\mathbf{q},\omega;z,z')V(\mathbf{q},\omega;z'), \tag{11}$$

where $V=V_{ex}+V_{in}$ is the total potential, with V_{ex} (V_{in}) as the external (induced) potential. The induced potential is further defined by

$$V_{in}(\mathbf{q},\omega;z) = \int dz' V_{ee}(q,z-z')n_{in}(\mathbf{q},\omega;z'), \tag{12}$$

where $V_{ee}(\cdots)$ is the 2D Fourier transform of the binary Coulombic interactions and is given by

$$V_{ee}(q,z-z') = \frac{2\pi e^2}{\epsilon_0 q} e^{-q|z-z'|}, \tag{13}$$

where ϵ_0 is the background dielectric constant of the medium in which the 2DEG is embedded. Solving Eqs. (10)–(12) together yields

$$V_{in}(\mathbf{q},\omega;z) = V_q \sum_{\substack{n\sigma \\ n'\sigma'}} \sum_{\mathbf{k}} \Lambda_{nn'}^{\sigma\sigma'}(\mathbf{k},\mathbf{k}') \times \int dz' e^{-q|z-z'|}\phi_{n'}^*(z')\phi_n(z') \times \langle n\sigma|V_{ex}+V_{in}|n'\sigma'\rangle\chi_{\sigma'}^*\chi_\sigma, \tag{14}$$

where $V_q=2\pi e^2/\epsilon_0 q$. Let us now take the matrix elements of both sides between the states $|m\sigma''\rangle$ and $|m'\sigma'''\rangle$. The result is

$$\langle m\sigma''|V_{in}|m'\sigma'''\rangle = V_q \sum_{\substack{n\sigma \\ n'\sigma'}} \sum_{\mathbf{k}} \Lambda_{nn'}^{\sigma\sigma'}(\mathbf{k},\mathbf{k}')F_{mm'nn'}(q) \times \langle n\sigma|V|n'\sigma'\rangle\chi_{\sigma''}^*\chi_{\sigma'''}\chi_{\sigma'}^*\chi_\sigma, \tag{15}$$

where the function $F_{mm'nn'}(q)$ is defined by

$$F_{mm'nn'}(q) = \int dz \int dz' \phi_m^*(z)\phi_{m'}(z)e^{-q|z-z'|}\phi_{n'}^*(z')\phi_n(z'). \tag{16}$$

We can cast Eq. (15) in the form

$$\langle \nu|V_{ex}|\nu'\rangle = \sum_{\mu\mu'} \left[\delta_{\mu\nu}\delta_{\mu'\nu'} - V_q \sum_{\vec{k}} \Lambda_{\mu\mu'}N_{\mu\mu'\nu\nu'} \right] \langle \mu|V|\mu'\rangle, \tag{17}$$

where

$$N_{\mu\mu'\nu\nu'} = F_{nn'mm'}M_{\sigma\sigma'\sigma''\sigma'''},$$

with

$$M_{\sigma\sigma'\sigma''\sigma'''} = \chi_\sigma^*\chi_{\sigma'}\chi_{\sigma''}^*\chi_{\sigma'''} \tag{18}$$

and $\mu \equiv n\sigma$, $\mu' \equiv n'\sigma'$, $\nu \equiv m\sigma''$, and $\nu' \equiv m'\sigma'''$. Since the external and total potentials are related such that

$$V_{ex}(z) = \int dz' \epsilon(z,z')V(z'), \tag{19}$$

we can deduce from Eq. (17) that the generalized nonlocal, dynamic dielectric function is given by

$$\epsilon_{\mu\mu'\nu\nu'} = \delta_{\mu\nu'}\delta_{\mu'\nu} - V_q \sum_{\mathbf{k}} \Lambda_{\mu\mu'}N_{\mu\mu'\nu\nu'}. \tag{20}$$

The matrix $\tilde{\epsilon}$ in Eq. (20) is symbolically written as follows:

$$\tilde{\epsilon}(\mathbf{q},\omega) = \begin{bmatrix} \epsilon_{++++} & \epsilon_{+++-} & \epsilon_{++-+} & \epsilon_{++--} \\ \epsilon_{+-++} & \epsilon_{+-+-} & \epsilon_{+--+} & \epsilon_{+---} \\ \epsilon_{-+++} & \epsilon_{-++-} & \epsilon_{-+-+} & \epsilon_{-+--} \\ \epsilon_{--++} & \epsilon_{--+-} & \epsilon_{---+} & \epsilon_{----} \end{bmatrix}. \tag{21}$$

We thus need to evaluate first all such $M_{\sigma\sigma'\sigma''\sigma'''}$ with $\sigma,\sigma',\sigma'',\sigma''' = \pm 1$. This is relegated to Appendix A for the sake of continuity.

Before we proceed further, it is important to specify that we are strictly concerned in this work with the case of a narrow quantum well where only the lowest (electric) subband is occupied and we ignore any excited subband. That implies that we are virtually confined to a purely 2DEG at very low temperature. This would then mean that the subband indices $n=n'=m=m'=0$ and hence the z coordinate drops out of consideration and hence $F_{nn'mm'}(q)=1$ and $N_{\mu\mu'\nu\nu'} \to M_{\sigma\sigma'\sigma''\sigma'''}$. This then allows us to cast Eq. (20) in the following form:

$$\epsilon_{\sigma\sigma'\sigma''\sigma'''} = \delta_{\sigma\sigma'''}\delta_{\sigma'\sigma''} - V_q \sum_{\mathbf{k}} \Lambda_{\sigma\sigma'}M_{\sigma\sigma'\sigma''\sigma'''}. \tag{22}$$

It is a simple matter to prove that here (see Appendix A)

$$M_{\sigma\sigma'\sigma''\sigma'''} = \begin{cases} +\frac{1}{2}(1+A), & \text{if } \sigma=\sigma' \text{ and } \sigma''=\sigma''', \\ +\frac{1}{2}(1-A), & \text{if } \sigma\neq\sigma' \text{ and } \sigma''\neq\sigma''', \\ +\frac{1}{2}iB, & \text{if } \sigma=\sigma' \text{ and } \sigma''\neq\sigma''', \\ -\frac{1}{2}iB, & \text{if } \sigma\neq\sigma' \text{ and } \sigma''=\sigma'''. \end{cases} \tag{23}$$

Given the fact that

$$\sum_{\mathbf{k}} \Lambda_{\sigma\sigma'} B = 0, \tag{24}$$

the matrix in Eq. (21) now assumes the following form:

$$\tilde{\epsilon}(\mathbf{q},\omega) = \begin{bmatrix} 1-\epsilon_{++} & 0 & 0 & \epsilon_{++} \\ 0 & 1-\epsilon_{+-} & \epsilon_{+-} & 0 \\ 0 & \epsilon_{-+} & 1-\epsilon_{-+} & 0 \\ \epsilon_{--} & 0 & 0 & 1-\epsilon_{--} \end{bmatrix}, \tag{25}$$

where $\epsilon_{\pm\pm}=(V_q/2)\Sigma_{\mathbf{k}}(1+A)\Lambda_{\pm\pm}$ refers to the intra-SO transitions and $\epsilon_{\pm\mp}=(V_q/2)\Sigma_{\mathbf{k}}(1-A)\Lambda_{\pm\mp}$ to the inter-SO transitions. As usual, the modes of the plasmon excitations are obtained by equating the determinant of the dielectric function matrix to zero. The result is that

$$|\tilde{\epsilon}| = (1-\epsilon_{++}-\epsilon_{--})(1-\epsilon_{+-}-\epsilon_{-+}) = 0 \tag{26}$$

furnishes the intra-SO (inter-SO) plasmons by equating the first (second) factor to zero in this equation. Notice that Eq. (26) is the exact expression obtained within the RPA, which demonstrates how the plasmons in a 2DEG can be achieved via electronic transistions in different spin channels. Since the inverse of the nonlocal, dynamic dielectric function serves many useful purposes, we give in Appendix B the quantity $\tilde{\epsilon}^{-1}(\mathbf{q},\omega)$.

We made some analytical diagnosis of Eq. (26) in the long-wavelength limit (i.e., $q\to 0$) at low temperature ($T\to 0$). We obtain

$$\omega = \omega_p \left[1 - \frac{\omega_- - \omega_+}{\omega_0} \right]^{1/2} \tag{27}$$

for the intra-SO plasmons and

$$\omega = \frac{\omega_p^2}{2\omega_0} \ln\left[\frac{\omega-\omega_-}{\omega+\omega_-}\frac{\omega+\omega_+}{\omega-\omega_+} \right] \tag{28}$$

for the inter-SO plasmons. Here $\omega_p=(2\pi n_e e^2 q/\epsilon_0 m^*)^{1/2}$ is the 2D screened plasmon frequency in the absence of the SOI, $\omega_0=8\pi n_e\hbar/m^*$, $\omega_\pm=4\alpha\sqrt{\pi n_\pm}/\hbar$, and the 2D charge density $n_e=n_+ + n_-$. Note that the second term inside the square brackets in Eq. (27) is exactly equal to $k_\alpha^2/(2\pi n_e)$, where k_α can be written such that $k_\alpha=\sqrt{\pi n_-}-\sqrt{\pi n_+}$. The electron density in different "spin channels," given by

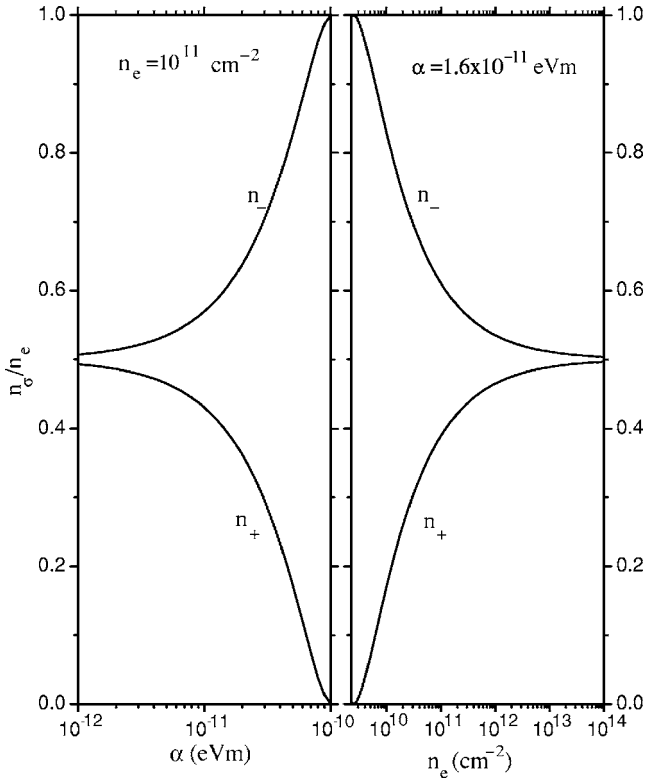

FIG. 2. Electron distribution in different spin channels as a function of the Rashba parameter α (left panel) and the 2D charge density n_e (right panel).

$$n_\pm = \frac{n_e}{2} \mp \frac{k_\alpha}{2\pi} k_F, \tag{29}$$

is obtained by imposing the condition of electron number conservation and reflects the different Fermi momenta for each branch in Fig. 1. Here the Fermi wave vector $k_F=\sqrt{2\pi n_e - k_\alpha^2}$. In addition, two "spin channels" are characterized by different effective Fermi vectors $k_F^\pm=(k_F\mp k_\alpha)$. In what follows, we solve exactly Eq. (26). We will see below that the exact inter-SO modes result in two explicit solutions, in agreement with Eq. (28), so that the SOI gives rise to *three* different collective (plasmon) modes for a given momentum transfer q.

III. ILLUSTRATIVE EXAMPLES OF PLASMON EXCITATIONS

This section is devoted to discuss our illustrative numerical examples of the plasmon excitations in a 2DEG in the presence of the spin-orbit interactions, computed at $T=0$ K. We do so by examining the influence of several parameters involved in the analytical results. These are, for instance, the Rashba parameter α, the 2D charge density n_e, and the propagation vector q.

Figure 2 illustrates the electron density distribution as a function of the Rashba parameter α (the left panel) and the total 2D electron density n_e (right panel). As is expected,[6] the electron distribution is different in different spin channels. It is clear from this figure that the electron density is greater in

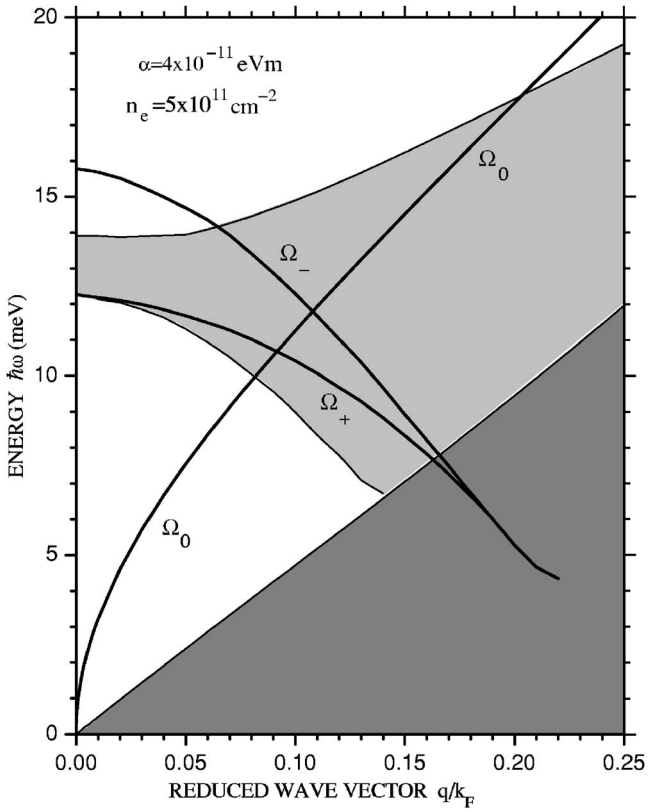

FIG. 3. The 2D plasmon energy as a function of the momentum transfer, q/k_F. The bold curves are the intra-SO (Ω_0) and inter-SO ($\Omega_\pm$) plasmons. We call attention to the intra-SO (dark shaded region) and inter-SO (light shaded region) single-particle excitations, which define the limits of the survival of the respective plasmons (bold curves). The material parameters are as listed inside the picture.

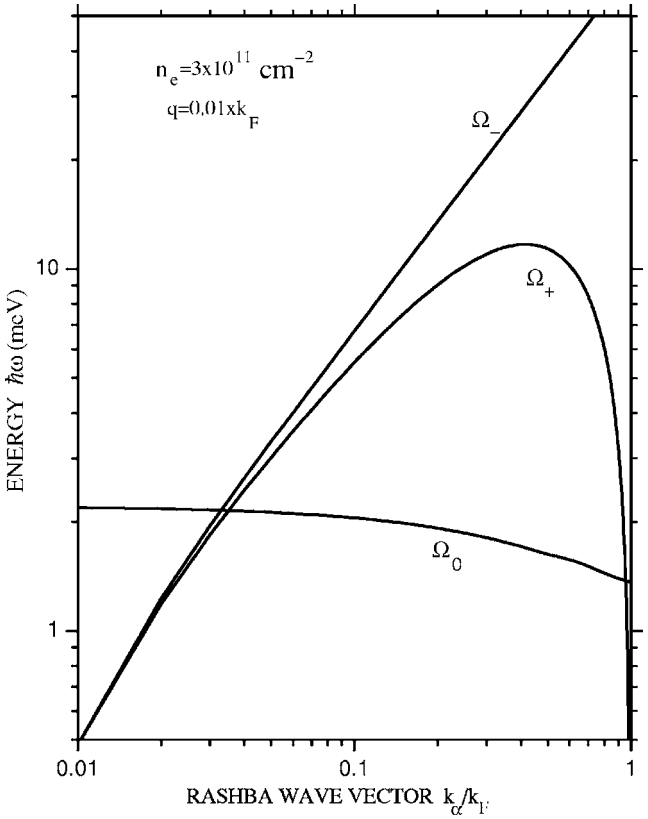

FIG. 4. The plasmon excitation energy as a function of (normalized) effective Rashba wave vector (k_α/k_F). The 2D charge density $n_e=3\times10^{11}$ cm^{-2} and the momentum transfer $q=0.01k_F$. Notice the logarithmic scale on both axes.

spin-down channel (n_-) because it has larger Fermi momentum.

Figure 3 depicts the energy dispersion of the intra-SO (Ω_0) and inter-SO ($\Omega_\pm$) plasmons as a function of the (normalized) momentum transfer q/k_F for the given value of the Rashba parameter ($\alpha=4.0\times10^{-11}$ eV m) and the 2D charge density ($n_e=5.0\times10^{11}$ cm^{-2}). As one can notice, the Rashba SOI gives rise to three plasmon branches (bold curves)—one intra-SO (Ω_0) and two inter-SO ($\Omega_\pm$) modes. The intra-SO plasmon branch that starts from the origin goes through the inter-SO SPE region quite unperturbed and will only decay into the intra-SO SPE region at short wavelength. Thus the lower (intra-SO) plasmon branch does *not* suffer from any Landau damping due to crossing the inter-SO SPE region. The upper, opticlike (inter-SO) plasmons start from the nonzero energy at the small (but finite) wave vector with negative group velocity—with the upper one (Ω_-) emerging from above the inter-SO SPE and the lower one (Ω_+) from just above the lower branch of the SPE region. While the lower plasmon mode (Ω_+) remains within the respective SPE throughout, the upper one (Ω_-) merges with the SPE at $q\simeq0.067k_F$. This clearly leads us to infer that except for the upper opticlike mode that remains a true plasmon in the range $0\lesssim q/k_F\lesssim0.067$, both inter-SO plasmon modes suffer from the Landau damping due to their merger with the respective SPE region. Thus lower intra-SO plasmon and the upper inter-SO plasmon in the range $0\lesssim q/k_F\lesssim0.067$ are the only true plasmon modes in the 2DEG with Rashba SOI and with only the lowest occupied subband. The upper (inter-SO) single-particle excitation spectrum attains a finite width even at the small (but nonzero) wave vector due to the nonzero Rashba parameter α. For $\alpha=0$, there exists neither the inter-SO plasmons nor the upper single-particle excitation region, just as is expected.

It is worth mentioning that we also performed similar computations as illustrated in Fig. 3, but for a different set of Rashba parameters ($\alpha=1.6\times10^{-11}$ eV m) and the 2D charge density ($n_e=1.0\times10^{11}$ cm^{-2}), within the same range of the momentum transfer q/k_F. It was observed that while the collective and single-particle excitations obey the similar propagation trend as in Fig. 3, the energy of both types of excitations decrease (by a factor of 5) to lie in the range specified by $0\leqslant\hbar\omega$ (meV) $\leqslant4$. The dominant parameter that brings about such an effect of reducing the energy of plasmon excitations seems to be the 2D charge density n_e rather than the Rashba parameter α.

Figure 4 shows the plasmon frequency as a function of the (normalized) effective Rashba wave vector (k_α/k_F) for the given 2D electron density (n_e) and the momentum transfer q. What becomes evident from this figure is that the spin splitting of the inter-SO, opticlike plasmons is degenerate at very

low value of α and increases almost linearly with increasing α. At higher values of k_α, the spin-down plasmon (Ω_-) energy continues to increase while the spin-up plasmon (Ω_+) energy attains a maximum and then decreases rapidly to a small but nonzero value. The intra-SO plasmon (Ω_0) energy is seen to be almost constant over a wide range of k_α except at a very high value where it starts decreasing gradually. In this sense, we remark that the inter-SO plasmons are stronger functions of α than their intra-SO counterpart. It is easy to show that $\hbar\Omega_0 \simeq \hbar\omega_p\left(1-\frac{k_\alpha^2}{4\pi n_e}\right)$, for $k_\alpha^2 \ll 2\pi n_e$, as is the case here [see Eq. (27)]. It is noteworthy that this figure demonstrates how the plasmon energy of both intra-SO and inter-SO modes varies as a function of the Rashba parametr (α), irrespective of the fact that not all of these plasmons survive the Landau damping in the whole range of ω-q space.

IV. CONCLUDING REMARKS

In summary, the 2D (intra-SO) plasmons in the presence of SOI can significantly differ from the usual 2D plasmons (ω_p) in the absence of SOI. It has been demonstrated that a 2DEG with SOI can give rise, via intra-SO and inter-SO electronic transitions, to *three* plasmon branches with frequencies in the THz regime (1 THz$\simeq$4 meV) (see, e.g., Fig. 3). The physical picture behind the existence of two inter-SO plasmons seems to be the fact that the $\pm$ transitions differ from the $\mp$ ones. The inter-SO plasmons are seen to propagate with negative group velocity throughout. However, it is most important to note that major parts of the opticlike, inter-SO plasmons remain Landau damped since they propagate within the respective single-particle excitation region. The intra-SO plasmon branch does *not* suffer from any Landau damping due to crossing the inter-SO SPE region; it will only decay into the respective single-particle regime at very short wavelength. The inter-SO plasmons ($\Omega_\pm$) are seen to observe a stronger dependence on the Rashba parameter α and the 2D charge density n_e than their intra-SO (Ω_0) counterpart. We hope the theoretical predictions in this paper will soon be verified through either inelastic light (or Raman) or inelastic electron scattering experiments. Currently, we have been investigating the effect of the SOI on plasmon excitations in a quasi-2DEG in the presence of a perpendicular magnetic field and in a quasi-1DEG both with and without an applied magnetic field and the results will be reported shortly.

ACKNOWLEDGMENTS

The work of M.S.K. was partially suported by CONACyT Grant No. SEP-2003-C02-42761. S.E.U. acknowledges support of NSF-IMC Grant No. 0336431.

APPENDIX A: THE FACTORS $M_{\sigma\sigma'\sigma''\sigma'''}$

The various factors $M_{\sigma\sigma'\sigma''\sigma'''}$ are evaluated and listed as follows:

$$4M_{++++} = 4M_{++--} = 4M_{--++} = 4M_{----} = (1+A)^2 + B^2, \tag{A1}$$

$$4M_{+++-} = 4M_{++-+} = 4M_{--+-} = 4M_{---+} = 2iB, \tag{A2}$$

$$4M_{+-+-} = 4M_{+---} = 4M_{-+--} = 4M_{-+-+} = (1-A)^2 + B^2, \tag{A3}$$

$$4M_{+-++} = 4M_{+---} = 4M_{-+++} = 4M_{-+--} = -2iB, \tag{A4}$$

where $A=(k+q\cos\theta)/|\mathbf{k}'|$ and $B=q\sin\theta/|\mathbf{k}'|$. Here θ is the angle between $\mathbf{k}$ and $\mathbf{q}$.

APPENDIX B: THE INVERSE OF $\tilde{\epsilon}(\mathbf{q},\omega)$ DERIVED IN EQ. (25)

A systematic calculation yields the inverse dielectric function given by,

$$\tilde{\epsilon}^{-1}(\mathbf{q},\omega) = \begin{bmatrix} 1+\epsilon^*_{++} & 0 & 0 & \epsilon^*_{++} \\ 0 & 1+\epsilon^*_{+-} & \epsilon^*_{+-} & 0 \\ 0 & \epsilon^*_{-+} & 1+\epsilon^*_{-+} & 0 \\ \epsilon^*_{--} & 0 & 0 & 1+\epsilon^*_{--} \end{bmatrix}, \tag{B1}$$

where

$$\epsilon^*_{++} = \frac{\epsilon_{++}}{1-\epsilon_{++}-\epsilon_{--}}, \tag{B2}$$

$$\epsilon^*_{--} = \frac{\epsilon_{--}}{1-\epsilon_{++}-\epsilon_{--}}, \tag{B3}$$

$$\epsilon^*_{+-} = \frac{\epsilon_{+-}}{1-\epsilon_{+-}-\epsilon_{-+}}, \tag{B4}$$

$$\epsilon^*_{-+} = \frac{\epsilon_{-+}}{1-\epsilon_{+-}-\epsilon_{-+}}. \tag{B5}$$

[1] For an extensive review of electronic, optical, and transport properties of systems of reduced dimensions, such as quantum wells, wires, dots, and modulated 2D systems, see M. S. Kushwaha, Surf. Sci. Rep. **41**, 1 (2001).

[2] For a recent review of the field of spintronics, see I. Zutic, J. Fabian, and S. Das Sarma, Rev. Mod. Phys. **76**, 323 (2004).

[3] S. Datta and B. Das, Appl. Phys. Lett. **56**, 665 (1990).

[4] E. I. Rashba, Sov. Phys. Solid State **2**, 1109 (1960).

[5] G. Lommer, F. Malcher, and U. Rossler, Phys. Rev. Lett. **60**, 728 (1988).

[6] J. Luo, H. Munekata, F. F. Fang, and P. J. Stiles, Phys. Rev. B **41**, 7685 (1990).
[7] P. F. Hopkins, K. L. Campman, G. Bellomi, A. C. Gossard, M. Sundaram, E. L. Yuh, and E. G. Gwinn, Appl. Phys. Lett. **64**, 348 (1994).
[8] C. L. Cates, G. Briceno, M. S. Sherwin, K. D. Maranowski, K. Campman, and A. C. Gossard, Physica E (Amsterdam) **2**, 463 (1998).
[9] R. Kohler, A. Tredicucci, F. Beltram, H. A. Beere, E. H. Linfield, A. G. Davies, D. A. Ritchie, R. C. Iotti, and F. Rossi, Nature (London) **417**, 156 (2002).
[10] L. I. Magarill, A. V. Chaplik, and M. V. Entin, JETP **92**, 153 (2001).
[11] E. G. Mishchenko and B. I. Halperin, Phys. Rev. B **68**, 045317 (2003).
[12] C. A. Ullrich and M. E. Flatte, Phys. Rev. B **68**, 235310 (2003). Note that this work considers the intersubband spin-density plasmons in a two-subband model, which differs from the purely intrasubband charge-density case studied in Refs. 13–15.
[13] W. Xu, Appl. Phys. Lett. **82**, 724 (2003).
[14] X. F. Wang, Phys. Rev. B **72**, 085317 (2005).
[15] G. Gumbs, Phys. Rev. B **72**, 165351 (2005).